

30° Partial Dislocations in Silicon: Absence of Electrically Active States

James R. Chelikowsky

*Corporate Research-Science Laboratories, Exxon Research and Engineering Company,
Linden, New Jersey 07036*

(Received 26 August 1982)

Partial dislocations are the most important intrinsic defects, other than point defects, in controlling the mechanical and electronic properties of silicon. From high-resolution electron-microscopy data, and a simple optimization procedure, a realistic geometry is presented for the 30° partial dislocation. Electronic structure calculations have been performed for this geometry and it has been established that no electrically active states are associated with this dislocation.

PACS numbers: 61.70.Ga, 71.55.Fr

One of the most crucial aspects of semiconductor physics is determining the role of defect states. These states, either extrinsic or intrinsic, can have drastic effects on the electrical properties of semiconductor devices. It is of some importance to ascertain the intrinsic defect concentration as a limit on the number of active states. Outside of intrinsic point defects, e.g., vacancies, interstitials, etc., the predominant intrinsic defects are associated with dissociated screw dislocations and dissociated 60° dislocations. The former consists of two 30° partial dislocations; the latter consists of one 90° and one 30° partial dislocation. Dislocations running in other directions may be thought of as kinked segments of these types.^{1,2} Thus, one can understand to a large extent how elemental defects affect the mechanical and electronic properties of tetrahedrally coordinated semiconductors by examining the 30° and 90° partial dislocations.

The 30° and 90° partial dislocations may lie either on the closely spaced (111) glide planes or on the more widely spaced (111) shuffle planes.³ The shuffle and glide configurations of the 30° partial dislocation differ in the presence or absence of a single column of atoms along the dislocation core. Recent evidence^{4,5} favors the glide model. I will concentrate on this model as it appears simpler to understand in terms of structure as compared with the 90° partial dislocation.

In Fig. 1, the atomic structure of the 30° partial dislocation is illustrated without any reconstruction of the core defect. In analogy to the problem of surface states, the most difficult aspect of obtaining a detailed picture of defect states is determining the atomic geometry. As an example, the 30° partial dislocation has certain characteristics which closely resemble the (100) surface of elemental silicon.⁷ Following the analogy

to this surface, one expects the 30° partial dislocation to reconstruct. Providing that the 30° partial dislocation does reconstruct, it might have a nonmetallic behavior in which the defect states have no associated free spins, but are still electrically active. Or, it might not have any strongly localized, i.e., electrically active, states associated with the defect. Quite apparently, the number of dangling bonds, recombination, luminescence, and even lattice friction⁸ will depend on the core geometry.

Unlike the case of surface structures, one has an experimental tool which can yield detailed information on atomic coordinates of extended defects: high-resolution electron microscopy.^{6,9} The atomic coordinates for the present calculation were taken from near-atomic-resolution-computed electron micrographs⁴ and then optimized to reduce bond-length and bond-angle deviations. This optimization procedure is necessary as the resolution of electron micrographs is at best 2 Å and the images depend sensitively

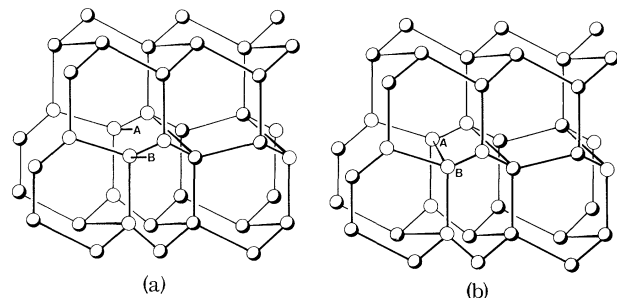


FIG. 1. Diagrammatic sketches of (a) unreconstructed 30° partial dislocation and (b) reconstructed 30° partial dislocation as in Ref. 6. The dislocation line runs in the $\langle 110 \rangle$ direction and joins the dangling bonds shown in (a) at A and B. The atoms (A,B) are bonded in pairs in the 30° partial reconstruction shown in (b).

on the electron optical parameters and specimen thickness.⁴

As in previous work,⁶ the defect is modeled by a supercell configuration. The artificial periodicity of the supercell allows one to use standard techniques to determine the electronic structure of the defect and to handle the geometry problem in a finite system. The first step of the optimization procedure is to use a matrix of fixed coordinates from electron-microscopy work. These initial coordinates were altered in a "mean-field" procedure. The coordinates of a given atom were examined and an attempt was made to minimize any bond-length deviations from the ideal crystalline bond length of that atom to its nearest neighbors. After the given atom was examined, its coordinates were saved for future use and then the procedure was repeated for another atom. When all the atoms in the matrix were examined, another matrix was set up with new coordinates and the procedure repeated. A number of iterations were performed until the coordinates converged. The advantages of this optimization procedure are as follows: (a) It preserves the initial symmetry of the system, (b) it is not dependent on the order in which the atomic coordinates are optimized, and (c) it is fast, easy, and accurate.

By analogy with surface reconstruction, one expects the 30° partial dislocation to "dimerize" or double the periodicity along the core axis. The most likely reconstruction is contrasted in Fig. 1 with the unreconstructed partial dislocation. Before considering the reconstructed model, the unreconstructed geometry was optimized. The unreconstructed partial dislocation was modeled with 48 atoms in a unit cell. Only a small perturbation of atomic coordinates was allowed, i.e., a few percent of a bond length, during each iteration. It was found in a few iterations that a very bulklike configuration could be achieved, except for the core axis which contains threefold-coordinated atoms. With no constraints on the bond angles, all the bond lengths in the unreconstructed model were found to be within 1%–2% of the ideal bond length. No further optimization of the model with respect to bond angles was performed as the bond angles without optimization were within 5–10 deg of the ideal values.¹⁰ A reconstructed model was then optimized by doubling the unit cell to contain 96 atoms and allowing a pairing reconstruction. No significant bond-length or bond-angle errors were found. Unlike the unreconstructed case, all atoms are tetrahedrally

coordinated as the core atoms rebond to become fourfold coordinated. Thus the 30° partial dislocation could be reconstructed to a nearly perfect bulklike configuration. The only significant deviations from the ideal crystalline state were in the bond angles, but even these deviations were small, i.e., typically 5 deg or less. Coordinates

TABLE I. Atomic coordinates (in angstroms) of 30° partial dislocation within a supercell configuration. There are two dislocations in the supercell with a center of inversion. The supercell is an orthorhombic unit cell ($a = 26.95 \text{ \AA}$, $b = 9.41 \text{ \AA}$, $c = 7.68 \text{ \AA}$, $\alpha = \beta = \gamma = 90^\circ$).

ATOM	x	y	z
1	13.41	-3.52	1.91
2	13.42	-3.50	5.75
3	10.10	-3.78	-0.02
4	10.07	-3.78	3.84
5	6.90	-3.80	1.92
6	6.83	-3.79	5.84
7	3.45	-3.72	0.18
8	3.39	-3.71	4.03
9	0.15	-3.55	2.22
10	0.15	-3.55	6.07
11	3.21	3.34	-0.10
12	3.21	3.34	3.76
13	6.55	3.24	1.90
14	6.51	3.24	5.76
15	10.00	3.24	0.00
16	10.03	3.26	3.84
17	11.31	2.73	1.90
18	11.32	2.74	5.75
19	7.75	2.52	-0.01
20	7.74	2.59	3.85
21	4.31	2.49	1.84
22	4.29	2.39	5.66
23	0.95	2.68	-0.29
24	0.95	2.68	3.55
25	2.38	-2.78	2.09
26	2.38	-2.78	5.96
27	5.68	-2.91	0.08
28	5.69	-3.16	3.85
29	9.06	-2.87	1.93
30	9.01	-2.88	5.77
31	12.23	-2.77	-0.01
32	12.23	-2.77	3.84
33	11.25	0.37	1.91
34	11.17	0.35	5.75
35	7.69	0.13	0.13
36	7.89	0.23	3.91
37	3.72	0.36	0.90
38	3.96	0.25	4.72
39	0.55	0.41	-0.96
40	0.55	0.41	2.88
41	2.74	-0.51	-1.06
42	2.70	-0.56	2.82
43	5.79	-0.80	1.17
44	5.75	-0.81	3.56
45	9.04	-0.51	1.97
46	8.98	-0.50	5.89
47	12.37	-0.42	-0.01
48	12.37	-0.42	3.85

for the model are presented in Table I.

One can compare this study with several existing models in the literature.¹¹⁻¹⁴ Perhaps the most extensive study of the 30° partial dislocation is that of Marklund.¹² Marklund used a valence force potential after Keating¹⁵ to determine atomic coordinates for both the 30° and 90° partial dislocations. Marklund found that a pairing reconstruction minimized the total energy. While in principle his approach should be more sophisticated than the present study, I appear to have achieved a geometry closer to an ideal silicon configuration and, hence, of lower energy. There are two possible reasons for this. First, I have an initial configuration determined from experiment. Second, the "mean-field" minimization procedure appears superior to the *ad hoc* method Marklund used.

In order to determine the existence of defect states in the 30° partial dislocation model, I undertook a realistic solution of the wave equation for the 96-atom supercell. A peripheral orbital method was used as described by Louie.¹⁶ With use of five orbitals¹⁷ per atom, a 480×480 matrix was diagonalized. Five *d* orbitals were included in a perturbative fashion. The potential used was semiempirical. Obviously, the large unit cell prohibits a routine self-consistent solution for determining the potential. However, this potential yields accurate spectra for the bulk and surface energy bands of silicon without self-consistency and should be equally accurate for the line defect.⁶

In order to determine the presence of defect states within the band gap, a local density-of-states calculation was performed for the unreconstructed and reconstructed cases. The density of states was examined on a defect core atom and on a bulklike atom. In Fig. 2, the gap-region density of states is illustrated. For the unreconstructed case, I find a one-dimensional band of dangling-bond states which propagate along the dislocation line. For the reconstructed case, I find no defect-associated states within the band gap. However, I do find an increase of state density near the band edges. It is quite probable that this density arises from band tails associated with the small bond-angle deviations associated with the partial dislocation.

From these results, it is clear that the 30° partial dislocation can reconstruct to eliminate any defect-associated states. This is a crucial result in several respects. While the picture of negligible strain energy associated with recon-

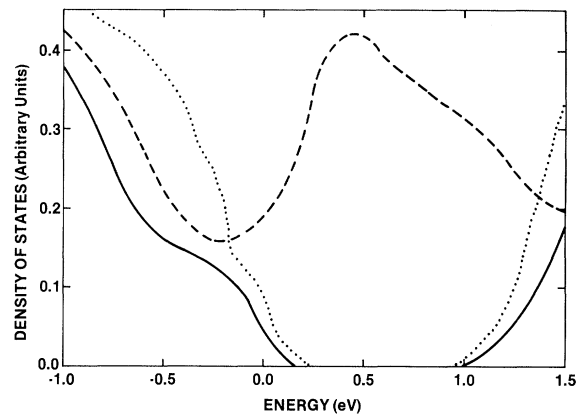


FIG. 2. Local density of states for the band-gap region of silicon showing the nature of defect states associated with the 30° partial dislocation. Three densities of states are indicated: bulk atom (solid line), unreconstructed partial core atom (dashed line), and reconstructed partial core atom (dotted line). The valence-band maximum is taken to be the energy zero.

structing the 30° partial dislocation is compatible with Marklund's work, my prediction of no states in the gap is in contradiction with some work which has suggested empty states in the upper part of the band gap.¹² I feel that my reconstruction model is clearly at variance with the existence of any localized states associated with the 30° partial dislocation as the bond lengths and angles are only slightly perturbed from a bulklike configuration. Moreover, my results clearly support some recent experimental findings which suggest that partial dislocations contribute electrically active states only at kinks.¹⁸

This reconstruction model also has some implication for other theoretical approaches. Some workers¹⁹ have speculated that Peierls transitions must be invoked to explain an absence of free-spin defects. The atomic geometry that I propose indicates that rebonding can eliminate any defect states without the need for more complex models.²⁰ This is similar to the case of surface reconstruction where traditional rebonding approaches have led to coherent pictures of semiconductor surfaces. With respect to theoretical models of soliton formation this work confirms speculation that soliton formation energies will be high for the 30° partial dislocation in that my reconstruction model is so bulklike.¹⁹

¹For a review of recent work, see J. Phys. (Paris),

Colloq. **40**, No. 6 (1979).

²The interpretation is in contrast to early theoretical work, e.g., W. Shockley, Phys. Rev. **91**, 228 (1953); W. T. Read, Jr., Philos. Mag. **98**, 116 (1954).

³J. P. Hirth and J. Lothe, *Theory of Dislocations* (McGraw-Hill, New York, 1968).

⁴A. Olsen and J. Spence, to be published; J. C. H. Spence, *Experimental High Resolution Electron Microscopy* (Oxford Univ. Press, Oxford, 1981).

⁵K. Wessel and H. Alexander, Philos. Mag. **35**, 1523 (1977).

⁶D. J. Chadi, J. Vac. Sci. Technol. **16**, 1290 (1979), and references therein.

⁷P. B. Hirsch, J. Phys. (Paris), Colloq. **40**, C6-27 (1979).

⁸P. B. Hirsch, J. Microsc. (Oxford) **118**, 3 (1980).

⁹J. E. Northrup, M. L. Cohen, J. R. Chelikowsky, J. Spence, and A. Olsen, Phys. Rev. **24**, 4623 (1981).

¹⁰As in previous work (Ref. 9), I include two 30° partial dislocations separated by a stacking fault. The two partial dislocations have opposite Burgers vectors. This means that there is no strain field outside the supercell.

¹¹S. Marklund, Phys. Status Solidi (b) **92**, 83 (1979).

¹²S. Marklund, Phys. Status Solidi (b) **100**, 77 (1980).

¹³M. J. Kirton, S. Brand, and M. Jaros, Philos. Mag. **42**, 577 (1980).

¹⁴M. J. Kirton and M. Jaros, J. Phys. C **14**, 2099 (1981).

¹⁵P. N. Keating, Phys. Rev. **145**, 637 (1966), and **149**, 674 (1966).

¹⁶S. G. Louie, Phys. Rev. B **22**, 1933 (1980).

¹⁷I use two *s*-symmetry orbitals to reproduce accurately the lower conduction bands. Details of the computation are the same as in Ref. 9.

¹⁸L. C. Kimerling, J. R. Patel, J. L. Benton, and P. E. Freeland, in Proceedings of the International Conference on Defects in Semiconductors, Osio, Japan, 1980 (to be published).

¹⁹R. Jones, in *Microscopy of Semiconducting Materials-1981*, edited by A. G. Cullis and D. C. Joy, IOP Conference Proceedings No. 60 (Institute of Physics, London, 1981), p. 45.

²⁰It has been suggested that the 90° partial dislocation need not involve a Peierls reconstruction [S. L. Altman, J. Phys. C **15**, 907 (1982)].

Evidence for a Soft Phonon Mode and a New Structure in Rare-Earth Metals under Pressure

W. A. Grosshans, Y. K. Vohra,^(a) and W. B. Holzapfel
*Experimentalphysik, Universität Gesamthochschule Paderborn, D-4790 Paderborn,
Federal Republic of Germany*

(Received 13 July 1982)

High-pressure x-ray diffraction experiments up to 30–40 GPa on lanthanum, praseodymium, and yttrium metals demonstrate that there is one more crystal structure in the regular rare-earth crystal-structure sequence. This structure results from a second-order phase transition in fcc phase and could be described by a zone-boundary soft phonon mode with $\vec{q} = (2\pi/a_0)(\frac{1}{2}, \frac{1}{2}, \frac{1}{2})$.

PACS numbers: 62.50.+p

The alkali metals, alkaline-earth metals, and rare earths as well as early transition metals show electron transfer from *s* to *d* bands under pressure. This *s*–*d* transfer results from relative lowering of *d*-like conduction states in comparison to *s* and *p* states which rise rapidly under compression. This electronic transition, which occurs over a wide range in volume, results in many structural transitions as well as in bulk-modulus anomalies in the group-IA to IIB elements.^{1–4} The rare-earth crystal-structure sequence hcp–Sm type–dhcp–fcc with decreasing atomic number and increasing pressure is one such example. In the course of *s*–*d* transfer in these materials, various band extrema pass

through the Fermi energy, thereby changing the connectivity of the Fermi surface. It is recognized^{5,6} that these topological changes of the Fermi surface can lead to anomalies in phonon frequencies and in some cases to phonon softening and structural phase transitions. Until recently, it was believed that the ultimate high-pressure phase of rare-earth metals is fcc. One earlier x-ray study⁷ on Pr, however, reported an orthorhombic distortion of the fcc lattice. Also, electrical resistivity measurements at low temperature and high pressures^{8,9} show resistance anomalies for Pr and La, in the fcc phase. The present x-ray diffraction measurements on La, Pr, and Y were intended to establish the microscopic